PROCEEDINGS OF SCIENCE

Exploring Quark Helicity Distributions with a 22 GeV Beam at Jefferson Lab

Cameron Cotton,[a,*] **Jefferson Smith**[a] **and Xiaochao Zheng**[a]

[a] *University of Virginia,*
Charlottesville, VA, USA

E-mail: cwc3cg@virginia.edu, qsc7ay@virginia.edu, xz5y@virginia.edu

Quark helicity distributions play a crucial role in our understanding of quantum chromodynamics (QCD) and the strong force, as well as in the study of nucleon structure. An energy upgrade of the electron beam at Jefferson Lab (JLab) from 11 to 22 GeV would provide a unique opportunity to advance our understanding of quark helicity distributions, allowing for nucleons to be probed at higher Bjorken x (x_{Bj}) than ever before. We present here an exploratory study of the impact such an upgrade would bring to our knowledge of the nucleon spin structure and quark helicity distributions through measurements of the virtual photon asymmetries A_1^n and A_1^p up to $x_{Bj} \approx 0.90$.

25th International Spin Physics Symposium (SPIN 2023)
24-29 September 2023
Durham, NC, USA

*Speaker

PoS(SPIN2023)159

1. Introduction

1.1 Physics Background

Studies of the spin structure of the nucleon first piqued the interest of the scientific community in the 1980s when the first measurements of the proton's polarized structure function g_1^p surprisingly appeared to show that the spin of quarks accounts for only a small fraction of the total spin of a nucleon, $12 \pm 17\%$ [1]. The latest results show that the spin of quarks accounts for approximately 30% of the total spin of a nucleon [2].

Since then, numerous experiments on polarized targets have been performed to improve our understanding of nucleon spin structure. The longitudinal virtual photon-nucleon asymmetry A_1, illustrated in Fig. 1, has been a key observable in many of these experiments. A_1 is given by

$$A_1(x_{Bj}, Q^2) = \frac{\sigma_{1/2} - \sigma_{3/2}}{\sigma_{1/2} + \sigma_{3/2}} = \frac{g_1(x_{Bj}, Q^2) - \frac{Q^2}{\nu^2} g_2(x_{Bj}, Q^2)}{F_1(x_{Bj}, Q^2)}, \tag{1.1}$$

where ν is the energy transfer in the target rest frame, Q^2 is the negative square of the 4-momentum carried by the exchanged virtual photon, $g_{1(2)}$ are the polarized structure functions, F_1 is an unpolarized structure function, and $\sigma_{1/2(3/2)}$ are the virtual photon absorption cross sections of the spin 1/2 and 3/2 photon-nucleon configurations, respectively [3].

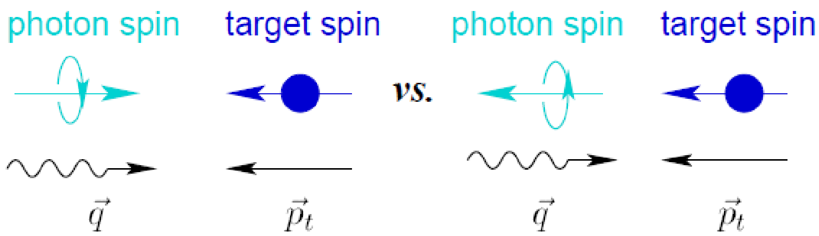

Figure 1: Reproduced from [3]. Visual representation of the longitudinal virtual photon asymmetry A_1. $\vec{q}$ is the virtual photon momentum and $\vec{p}_t$ is the momentum of the target nucleon.

We cannot directly control the polarization of the virtual photon, therefore A_1 must be determined from a linear combination of the electron-nucleon asymmetries $A_\parallel$ and $A_\perp$. These asymmetries can be obtained by changing the relative direction between the polarizations of the electron beam and the target material. $A_\parallel$ and $A_\perp$ are defined as:

$$A_\parallel = \frac{\sigma_{\downarrow\Uparrow} - \sigma_{\uparrow\Uparrow}}{\sigma_{\downarrow\Uparrow} + \sigma_{\uparrow\Uparrow}} \text{ and} \tag{1.2}$$

$$A_\perp = \frac{\sigma_{\downarrow\Rightarrow} - \sigma_{\uparrow\Rightarrow}}{\sigma_{\downarrow\Rightarrow} + \sigma_{\uparrow\Rightarrow}}. \tag{1.3}$$

These can be combined with kinematic factors to determine A_1 as

$$A_1 = \frac{1}{D(1+\eta\xi)} A_\parallel - \frac{\eta}{d(1+\eta\xi)} A_\perp, \tag{1.4}$$

where $D = \frac{1-(1-y)\epsilon}{1+\epsilon R}$, $\eta = \frac{\epsilon\sqrt{Q^2}}{E-E'\epsilon}$, $\xi = \eta(1+\epsilon)/(2\epsilon)$, $d = D\sqrt{2\epsilon/(1+\epsilon)}$, $\epsilon = 1/[1+2(1+\nu^2/Q^2)\tan^2(\theta/2)]$, $y = \frac{\nu}{E}$, E is the initial state energy of the electron, E' is the final state energy of the electron, θ is the electron scattering angle, and $R = \frac{\sigma_L}{\sigma_T}$, the ratio of the longitudinal to transverse virtual photon cross sections. To get from the measured A_1 for a given target to A_1^n and A_1^p, we must account for the rest of the target. For example, for A_1^n, a ^{3}He target is often used because a free neutron target does not exist [4]. Therefore, we must determine A_1^n from the measured value for $A_1^{^3\text{He}}$. To approximate this, we use the equation [3]

$$A_1^n = \frac{F_2^{^3\text{He}}}{P_n F_2^n(1+\frac{0.056}{P_n})}\left(A_1^{^3\text{He}} - 2\frac{F_2^p}{F_2^{^3\text{He}}}P_p(1-\frac{0.014}{2P_p})A_1^p\right), \tag{1.5}$$

where F_2 is an unpolarized structure function, and $P_n = 0.86 \pm 0.02$ and $P_p = -0.028 \pm 0.004$ are the effective neutron (proton) polarizations in ^{3}He [5]. To measure A_1^p, an NH_3 target [6] was assumed for this study. To determine the expected uncertainty for A_1^p from the uncertainty of $A_1^{NH_3}$, one can scale the uncertainty projected for the NH_3 target as

$$dA^p = dA^{NH_3}\frac{10F_2^p + 7F_2^n}{3F_2^p} \tag{1.6}$$

to account for the dilution from the nitrogen in NH_3. For this exploratory study, the free nucleon structure functions were used without additional nuclear corrections applied. Finally, as this study provided projections for both A_1^n and A_1^p, a flavor decomposition was performed to obtain $\Delta u/u$ and $\Delta d/d$, the ratio of the polarized quark distribution functions over the unpolarized quark distribution functions, using the equations

$$\frac{\Delta u + \Delta\bar{u}}{u+\bar{u}} = \frac{4}{15}\frac{g_1^p}{F_1^p}(4+\frac{d+\bar{d}}{u+\bar{u}}) - \frac{1}{15}\frac{g_1^n}{F_1^n}(1+4\frac{d+\bar{d}}{u+\bar{u}}) \text{ and} \tag{1.7}$$

$$\frac{\Delta d + \Delta\bar{d}}{d+\bar{d}} = \frac{4}{15}\frac{g_1^n}{F_1^n}(4+\frac{u+\bar{u}}{d+\bar{d}}) - \frac{1}{15}\frac{g_1^p}{F_1^p}(1+4\frac{u+\bar{u}}{d+\bar{d}}). \tag{1.8}$$

In this analysis, the anti-quark terms ($\bar{d}$ and $\bar{u}$) were taken to be negligible as we are most concerned with PDFs at large x_{Bj} where these terms are small. The values and uncertainties for $\frac{d}{u}$ were obtained using the Hessian-based *CJ15NLO* PDF set [7].

1.2 Jefferson Lab 22 GeV Upgrade

Jefferson Lab is home to the Continuous Electron Beam Accelerator Facility (CEBAF) [8]. This facility produces a high luminosity (100's of μA) electron beam of energies up to 12 GeV for simultaneous use in 4 experimental halls. Although CEBAF is currently limited to delivering beams with energies of up to 12 GeV, the accelerator tunnel was designed to handle beam energies of up to 22 GeV without suffering from significant energy loss due to synchrotron radiation. Since an upgrade to 22 GeV is technically feasible, efforts are underway to assess the scientific impact of such an upgrade and determine a method to optimize its execution from an accelerator science perspective [9]. At present, the most promising solution to elevate the beam energy involves the substitution of the two highest energy arcs with Fixed Field Alternating Gradient (FFA) arcs as shown in Fig. 2.

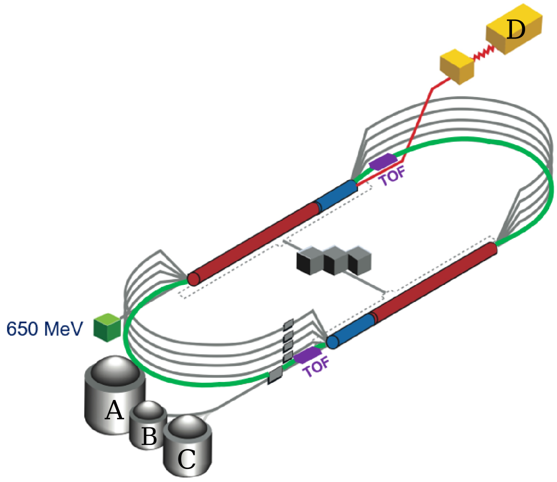

Figure 2: Adapted from [9]. CEBAF with the two highest energy arcs, Arc 9 and Arc A, replaced by a pair of FFA arcs (green).

These FFA arcs enable the accelerator to support multiple passes of the beam through a single physical arc, allowing for a doubling of the number of passes without requiring a corresponding doubling of physical arcs and the associated need to enlarge the tunnel to accommodate them.

2. Simulation and Analysis

2.1 Overview

The goal of this investigation was to perform impact studies of two potential 22 GeV inclusive Deep Inelastic Scattering (DIS) experiments in Halls B and C that could be used to extract the longitudinal virtual photon-nucleon asymmetries A_1^p and A_1^n. These two measurements could then be combined to extract the polarized quark distribution functions $\Delta q/q$.

2.2 A_1^p

To determine the expected measurement uncertainties for an A_1^p experiment at 22 GeV in Hall B, simulations were conducted using the CLASDIS event generator [10] and analyzed to account for specific conditions expected during the experiment. In our simulation, 10^7 DIS events were generated, and final results were binned in x_{Bj} in the range $0.05 < x_{Bj} < 0.90$, integrating over all Q^2 and $W^2 > 4\,\text{GeV}^2$, where W^2 is the invariant mass of the final state given by $W^2 = M^2+2M\nu+Q^2$ and M is the nucleon mass. The data were analyzed assuming the experiment would run for 30 days at 100% beam efficiency using the existing configuration of the CEBAF Large Acceptance Spectrometer (CLAS12), taking into account the present luminosity and acceptance constraints (Fig. 3). Although a luminosity upgrade of the CLAS12 spectrometer is anticipated in the near future, the current luminosity of $10^{35}\text{cm}^{-1}\text{s}^{-1}$ was used for the projections to provide a conservative estimate. In this analysis, an NH_3 target was used with nitrogen dilution estimated using Eq. 1.6, and the product of the beam and target polarization (P_bP_t) was taken to be 0.5 or 50%.

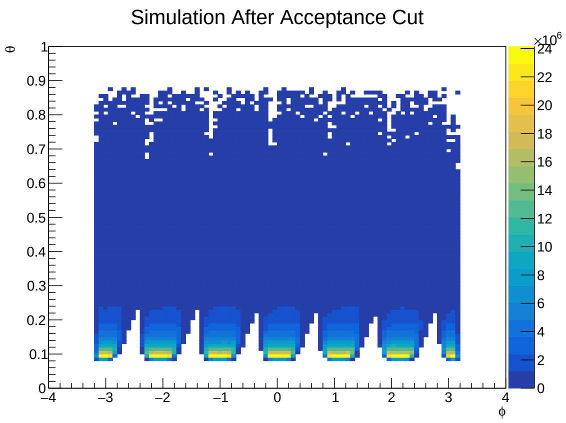

Figure 3: Distribution of simulated events in θ (polar angle) and ϕ (azimuthal angle) after CLAS12 acceptance cuts are applied.

For each bin in x_{Bj}, we first determine the raw statistical uncertainty of $A^{\mathrm{NH_3}}_{\parallel raw}$ and $A^{\mathrm{NH_3}}_{\perp raw}$ given by

$$dA^{\mathrm{NH_3}}_{\parallel(\perp)raw} = \frac{1}{\sqrt{N_{\parallel(\perp)}}}, \tag{2.1}$$

where $N_{\parallel(\perp)}$ is the estimated total number of events from the simulation in a given x_{Bj} bin for the longitudinal (transverse) $\mathrm{NH_3}$ polarization configuration. The $\mathrm{NH_3}$ target in CLAS can currently only be configured such that its polarization is longitudinal relative to the beam direction, therefore any uncertainty originating from the $A_\perp$ term was not addressed in this study. The raw uncertainties are then corrected to account for the beam and target polarizations, taking

$$dA^{\mathrm{NH_3}}_{\parallel(\perp)phys} = \frac{dA^{\mathrm{NH_3}}_{\parallel(\perp)raw}}{P_b P_t}. \tag{2.2}$$

Next, Eq. 1.6 is applied to convert from $dA^{\mathrm{NH_3}}_{\parallel phys}$ to $dA^{p}_{\parallel phys}$. Finally, Eq. 1.4 is applied to determine dA^p_1 from $dA^p_{\parallel phys}$ for each bin, using the values for D, η, and ξ at their centroids.

2.3 A^n_1

Similarly, to determine the expected measurement uncertainties for an A^n_1 experiment at 22 GeV in Hall C, simulations were conducted using the mc-single-arm event generator [11] and analyzed to account for particular experimental conditions. Unlike the CLASDIS event generator, the mc-single-arm event generator does not have a built-in cross-section model it uses to weigh events, so version 0.995 of the F1F221 model was used for this purpose [12]. For the A^n_1 projections, both of the small acceptance spectrometers that are currently present in Hall C, the High Momentum Spectrometer (HMS) and the Super High Momentum Spectrometer (SHMS), were simulated to collect simultaneous inclusive measurements for 30 days while set to angles of 30° and 20°, respectively. For this analysis, an electron beam with a longitudinal polarization of $P_b = 0.85$ and a current of 30μA was assumed, along with a 40 cm ^{3}He target with a polarization of $P_t = 0.5$ and a density of 10 amg. A dilution of 0.1 or 10% due to unpolarized nitrogen (N_2) in the target was assumed. To correct for this dilution, we define $f_{N_2} = 1 - 0.1 = 0.9$.

The process to determine A_1^n starting from $dA^{^3He}_{\parallel(\perp)raw}$ is similar to the process to determine A_1^p. The first difference is that, since the ^{3}He target can be put in both longitudinal and transversely polarized states, the term $A_\perp$ is not neglected and the runtime is optimally divided between the two configurations to minimize uncertainty. Additionally, in place of Eq. 2.2, the relation

$$dA^{^3\mathrm{He}}_{\parallel(\perp)phys} = \frac{dA^{^3\mathrm{He}}_{\parallel(\perp)raw}}{P_b P_t f_{N_2}} \tag{2.3}$$

is used to account for nitrogen dilution in the polarized ^{3}He target cell. Finally, as we are now extracting A_1^n from ^{3}He, Eq. 1.5 is used to propagate uncertainty from $A_1^{^3\mathrm{He}}$ to A_1^n.

3. Projected Results

Once simulations were completed to estimate the total number of events that are expected to be measured during the 30-day A_1^p and A_1^n experiments described in the previous section, our events were binned in x_{Bj}, physics corrections were applied, and statistical uncertainties were propagated from the raw number of events to A_1^p and A_1^n as previously discussed. As shown in Fig. 4, even a conservative estimate of the statistics that would be achieved for the short 30-day A_1^p and A_1^n experiments at 22 GeV would allow for competitive measurements of these quantities at larger x_{Bj} than is presently accessible, up from around $x_{Bj} = 0.75$ to approximately 0.90 at 22 GeV.

We then proceeded to extract the quark polarizations using Eqs. 1.7 and 1.8, see Fig. 5. While the precision for $\Delta u/u$ is high up to $x_{Bj} = 0.90$, we see that higher statistics are needed for the measurement of $\Delta d/d$ to determine whether it remains negative as indicated by existing data. This is due to the increasingly small probability of finding the down quark in the proton in the valence quark region, i.e., the smaller value of d/u in Eq. (1.8). Measurements of higher statistics can be achieved by a longer run time or with a large acceptance device such as SoLID [13], planned for Hall A of JLab. Nevertheless, the precision achieved for A_1^n using the conservative estimate presented here is already sufficient to distinguish between various theoretical predictions at large x_{Bj}.

4. Summary

We provide a first impact study of the possible 22 GeV energy upgrade of JLab on the nucleon valence quark spin structure. Using conservative running conditions, we found that the measurement of the virtual photon asymmetries $A_1^{p,n}$ can be extended to $x_{Bj} \approx 0.9$ straightforwardly. Furthermore, the quark polarizations can be extracted utilizing unpolarized PDFs as inputs. Higher statistics (with longer running or with the planned SoLID device) would further improve our knowledge of polarized light quark PDFs at large x_{Bj} and shed light on the QCD dynamics that determine the large x_{Bj} behavior of the polarized light quark PDFs.

Acknowledgments

We would like to express our gratitude for the feedback and suggestions from H. Avakian, J.-P. Chen, A. Deur, S. Kuhn, and D. Nguyen. This work was supported by the U.S. Department of Energy under Award number DE-SC0014434.

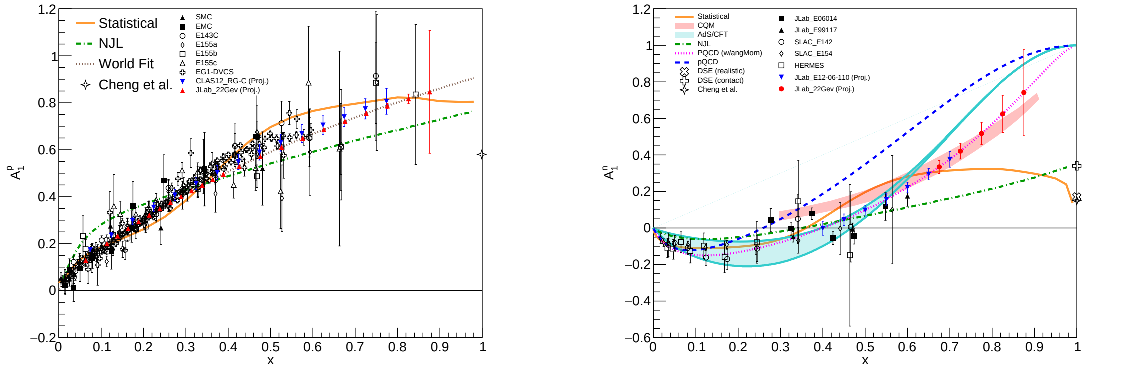

(a) Projected statistical uncertainties for the simulated 22 GeV A_1^p experiment are shown in red with data points arbitrarily placed on a previous world fit. The large increase in the statistical uncertainty for the largest x_{Bj} point should be examined more closely in future studies. Projections for the CLAS12 RG-C A_1^p measurement are given in blue. World data from SMC [14], EMC [1], CLAS EG1-DVCS [15], and SLAC E143 [16] and E155 [17] are shown alongside predictions from a Nambu–Jona-Lasinio (NJL) type model [18], a statistical model [19], a recent study by Cheng et al. [20], and a fit to the world data [21].

(b) Projected statistical uncertainties for the simulated 22 GeV A_1^n experiment are given in red with data points arbitrarily placed on one of the models. Projections for the 12 GeV A_1^n experiment are given in blue [22]. Results from SLAC E142 [23] and E154 [24], HERMES [25], and E99-117 [26] and E06-014 [21] from JLab are shown alongside predictions from perturbative QCD (pQCD) [27], a statistical quark model [19], a constituent quark model [28], a pQCD parameterization including angular momentum [29], an NLJ model [18], the Dyson-Schwinger equation [30], a recent study by Cheng et al. [20], and Light-Front Holographic QCD (LFHQCD), labeled AdS/CFT [31].

Figure 4: 22 GeV Projections for A_1^p and A_1^n

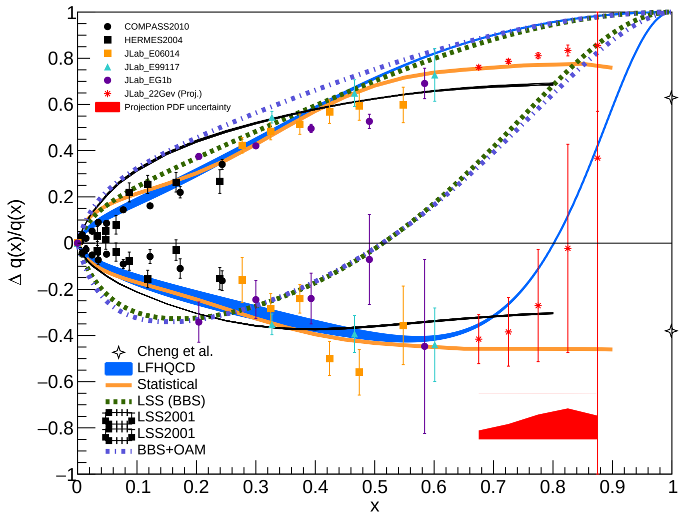

Figure 5: Projected uncertainties for $\Delta u/u$ and $\Delta d/d$ using *CJ15NLO* [7] and projected statistical uncertainties from possible 22 GeV A_1^p and A_1^n experiments. World data from COMPASS [32], HERMES [33], and JLab's EG1b [34], E99-117 [26] and E06-014 [21] are shown alongside theoretical predictions from a recent study by Cheng et al. [20], LFHQCD [31], a statistical quark model [19], and pQCD [35] [29].

References

[1] European Muon collaboration, *A Measurement of the Spin Asymmetry and Determination of the Structure Function g(1) in Deep Inelastic Muon-Proton Scattering*, Phys. Lett. B **206** (1988) 364.

[2] S.E. Kuhn, J.P. Chen and E. Leader, *Spin Structure of the Nucleon - Status and Recent Results*, Prog. Part. Nucl. Phys. **63** (2009) 1 [0812.3535].

[3] X. Zheng, *Precision Measurement of Neutron Spin Asymmetry A_1^n at Large x_{bj} Using CEBAF at 5.7 GeV*, Ph.D. thesis, Massachusetts Inst. of Technology (MIT), Cambridge, MA (United States), 2002. 10.2172/824895.

[4] J. Singh, P.A.M. Dolph, W.A. Tobias, T.D. Averett, A. Kelleher, K.E. Mooney et al., *Development of high-performance alkali-hybrid polarized ^{3}He targets for electron scattering*, Phys. Rev. C **91** (2015) 055205 [1309.4004].

[5] C. Ciofi degli Atti, S. Scopetta, E. Pace and G. Salme, *Nuclear effects in deep inelastic scattering of polarized electrons off polarized He-3 and the neutron spin structure functions*, Phys. Rev. C **48** (1993) R968 [nucl-th/9303016].

[6] W. Meyer, *Ammonia as a polarized solid target material: A review*, Nucl. Instrum. Meth. A **526** (2004) 12.

[7] Jefferson Lab Angular Momentum (JAM) collaboration, *Polarized antimatter in the proton from a global QCD analysis*, Phys. Rev. D **106** (2022) L031502 [2202.03372].

[8] C.W. Leemann, D.R. Douglas and G.A. Krafft, *The Continuous Electron Beam Accelerator Facility: CEBAF at the Jefferson Laboratory*, Ann. Rev. Nucl. Part. Sci. **51** (2001) 413.

[9] A. Accardi et al., *Strong Interaction Physics at the Luminosity Frontier with 22 GeV Electrons at Jefferson Lab*, 2306.09360.

[10] CLAS Collaboration, "CLASDIS." https://github.com/JeffersonLab/clasdis, 2023.

[11] Jefferson Lab, "mc-single-arm." https://github.com/JeffersonLab/mc-single-arm, 2023.

[12] P.E. Bosted and V. Mamyan, *Empirical Fit to electron-nucleus scattering*, 1203.2262.

[13] Jefferson Lab SoLID collaboration, *The solenoidal large intensity device (SoLID) for JLab 12 GeV*, J. Phys. G **50** (2023) 110501 [2209.13357].

[14] Spin Muon collaboration, *Spin asymmetries A(1) and structure functions g1 of the proton and the deuteron from polarized high-energy muon scattering*, Phys. Rev. D **58** (1998) 112001.

[15] CLAS collaboration, *Precision measurements of g_1 of the proton and the deuteron with 6 GeV electrons*, Phys. Rev. C **90** (2014) 025212 [1404.6231].

[16] E143 collaboration, *Measurements of the proton and deuteron spin structure functions g(1) and g(2)*, Phys. Rev. D **58** (1998) 112003 [hep-ph/9802357].

[17] E155 collaboration, *Measurement of the proton and deuteron spin structure functions g(2) and asymmetry A(2)*, Phys. Lett. B **458** (1999) 529 [hep-ex/9901006].

[18] I.C. Cloet, W. Bentz and A.W. Thomas, *Nucleon quark distributions in a covariant quark-diquark model*, Phys. Lett. B **621** (2005) 246 [hep-ph/0504229].

[19] C. Bourrely and J. Soffer, *New developments in the statistical approach of parton distributions: tests and predictions up to LHC energies*, Nucl. Phys. A **941** (2015) 307 [1502.02517].

[20] P. Cheng, Y. Yu, H.-Y. Xing, C. Chen, Z.-F. Cui and C.D. Roberts, *Perspective on polarised parton distribution functions and proton spin*, Phys. Lett. B **844** (2023) 138074 [2304.12469].

[21] Jefferson Lab Hall A collaboration, *Measurements of d_2^n and A_1^n: Probing the neutron spin structure*, Phys. Rev. D **94** (2016) 052003 [1603.03612].

[22] X. Zheng, M. Chen and C. Hedinger, “Measurement of the Neutron Spin Asymmetry in the Deep Valence Quark Region at Jefferson Lab 12 GeV.” this proceedings, 2024.

[23] E142 collaboration, *Deep inelastic scattering of polarized electrons by polarized He-3 and the study of the neutron spin structure*, Phys. Rev. D **54** (1996) 6620 [hep-ex/9610007].

[24] E154 collaboration, *Measurement of the neutron spin structure function g2(n) and asymmetry A2(n)*, Phys. Lett. B **404** (1997) 377 [hep-ex/9705017].

[25] HERMES collaboration, *Measurement of the neutron spin structure function g1(n) with a polarized He-3 internal target*, Phys. Lett. B **404** (1997) 383 [hep-ex/9703005].

[26] Jefferson Lab Hall A collaboration, *Precision measurement of the neutron spin asymmetries and spin-dependent structure functions in the valence quark region*, Phys. Rev. C **70** (2004) 065207 [nucl-ex/0405006].

[27] E. Leader, A.V. Sidorov and D.B. Stamenov, *NLO QCD analysis of polarized deep inelastic scattering*, Int. J. Mod. Phys. A **13** (1998) 5573 [hep-ph/9708335].

[28] N. Isgur, *Valence quark spin distribution functions*, Phys. Rev. D **59** (1999) 034013 [hep-ph/9809255].

[29] H. Avakian, S.J. Brodsky, A. Deur and F. Yuan, *Effect of Orbital Angular Momentum on Valence-Quark Helicity Distributions*, Phys. Rev. Lett. **99** (2007) 082001 [0705.1553].

[30] C.D. Roberts, R.J. Holt and S.M. Schmidt, *Nucleon spin structure at very high-x*, Phys. Lett. B **727** (2013) 249 [1308.1236].

[31] T. Liu, R.S. Sufian, G.F. de Téramond, H.G. Dosch, S.J. Brodsky and A. Deur, *Unified Description of Polarized and Unpolarized Quark Distributions in the Proton*, *Phys. Rev. Lett.* **124** (2020) 082003 [1909.13818].

[32] COMPASS collaboration, *Quark helicity distributions from longitudinal spin asymmetries in muon-proton and muon-deuteron scattering*, *Phys. Lett. B* **693** (2010) 227 [1007.4061].

[33] HERMES collaboration, *Flavor decomposition of the sea quark helicity distributions in the nucleon from semiinclusive deep inelastic scattering*, *Phys. Rev. Lett.* **92** (2004) 012005 [hep-ex/0307064].

[34] CLAS collaboration, *Measurement of the x- and Q**2-dependence of the asymmetry A(1) on the nucleon*, *Phys. Lett. B* **641** (2006) 11 [nucl-ex/0605028].

[35] S.J. Brodsky, M. Burkardt and I. Schmidt, *Perturbative QCD constraints on the shape of polarized quark and gluon distributions*, *Nucl. Phys. B* **441** (1995) 197 [hep-ph/9401328].